Supporting Information

Single-crystal Pt-decorated WO_3 Ultrathin Films: A Platform for Sub-ppm Hydrogen Sensing at Room Temperature

Giordano Mattoni,*,† Bas de Jong,† Nicola Manca,† Massimo Tomellini,‡ and Andrea D. Caviglia†

†*Kavli Institute of Nanoscience, Delft University of Technology, 2628 CJ Delft, The Netherlands*

‡*Dipartimento di Scienze e Tecnologie Chimiche, Università di Roma Tor Vergata, via della Ricerca Scientifica 1, 00133 Roma, Italy*

¶*Istituto di Struttura della Materia, CNR, via Fosso del Cavaliere 100, 00133 Roma, Italy*

E-mail: g.mattoni@tudelft.nl

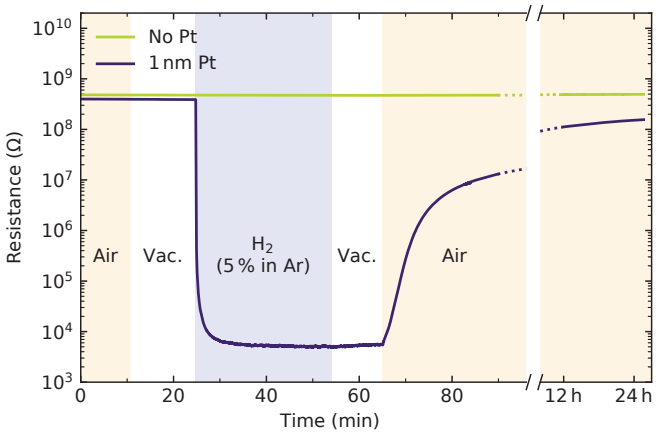

Figure S1: **WO_3 response with and without catalyst.** We compare the resistance change of two WO_3 devices, one without catalyst and one with 1 nm of Pt. The samples have comparable resistance in pristine conditions. Upon exposure to 5 % H_2 in Ar carrier gas, vacuum, and air the bare WO_3 sample shows no change in resistance, while the one with Pt shows a sharp drop and recovery. This underscores the crucial role of the noble metal in catalysing the hydrogen intercalation process.

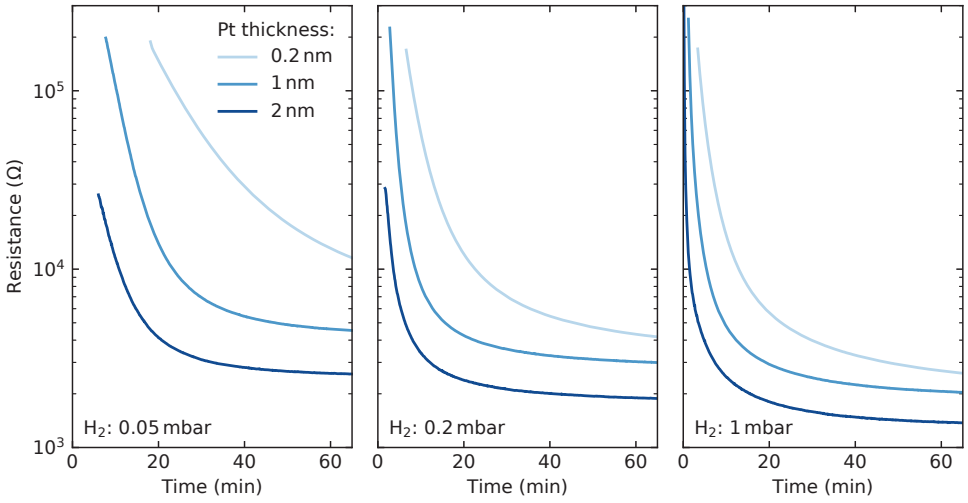

Figure S2: **Influence of the amount of Pt catalyst.** We compare the sensing response of three different WO_3 devices where the equivalent amount of Pt catalyst is in the range 0.2–2 nm. The measurements are performed simultaneously using a four-probe configuration which allows to measure resistance values in the range 1×10^3–$2 \times 10^5\,\Omega$. The temperature is fixed at 65 °C, and the devices are initially in the high-resistance undoped state (this value is above the instrumental resolution in the range selected for the measurement). At $t = 0$, we expose the devices to a 20 % H_2/Ar gas blend and measure the resistance drop over time. The experiment is repeated for different values of H_2 partial pressure in the range 0.05–1 mbar. The data shows that at all pressures a higher amount of Pt catalyst determines a faster response of WO_3 to H_2 gas.

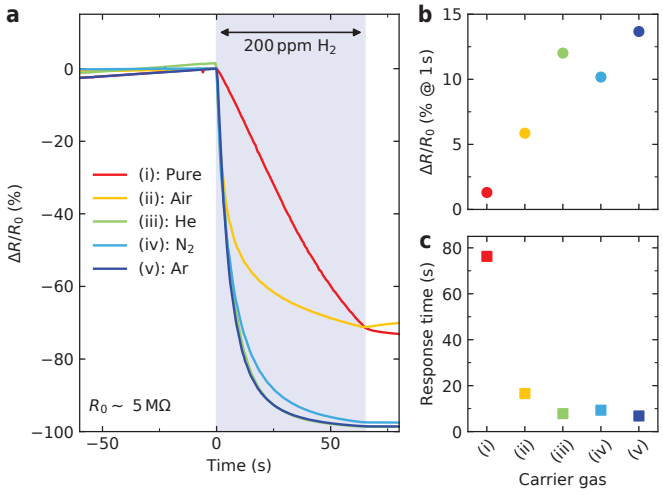

Figure S3: **Hydrogen intercalation with different carrier gases.** (a) At $t = 0$ the material is exposed to 200 ppm of H_2 in the atmosphere of a carrier gas at a total pressure of 1 bar. The used gases are: (i) pure, (ii) air, (iii) He, (iv) N_2, (v) Ar. In the case labelled as "pure", a low-pressure (1 mbar) gas blend 20 % H_2 in Ar is used. (b) Percentage variation after 1 s exposure and (c) exponential response time. The intercalation rates in He, N_2 and Ar carrying gases are comparable, indicating that these gases do not modify the intercalation process. We observe a reduced intercalation rate in air. This can be related to the recombination of H_2 and O_2 molecules to form water on the surface of WO_3, thus reducing the H_2 concentration entering the WO_3 lattice, as previously reported by Zhu et. al (ref.[36] of the main text). Interestingly, an even lower intercalation rate is observed when using "pure" hydrogen. This data highlights the versatility of our WO_3 device, which can be used for H_2 sensing in several gaseous atmospheres.

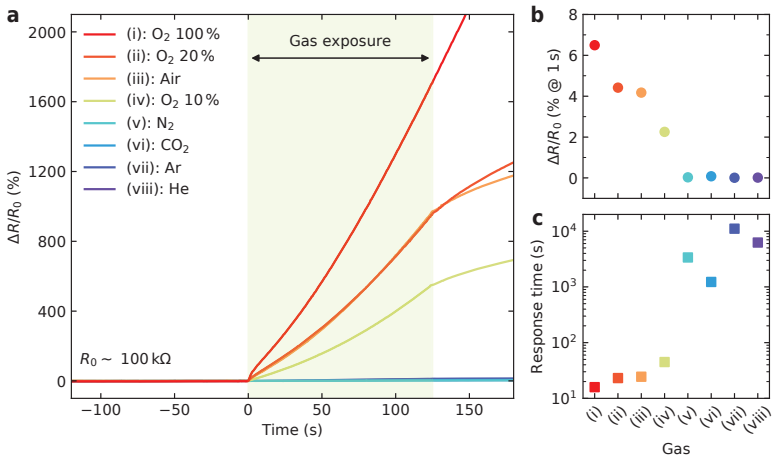

Figure S4: **Recovery in different gases.** (a) Before the measurement, the WO_3 device is doped with H_2 to reach an initial state with $R_0 \sim 100\,\mathrm{k\Omega}$, value that is approximately constant in vacuum for the few minutes prior to the gas exposure. At $t = 0$, the indicated gas is introduced in the sample chamber with a pressure of 1 bar. The used gases are: (i) O_2 100 %, (ii) O_2 20 %, (iii) air, (iv) O_2 10 %, (v) N_2, (vi) CO_2, (vii) Ar, (viii) He. At $t = 0$, the indicated gas is introduced in the sample chamber with a pressure of 1 bar. Partial pressures of oxygen are obtained by mixing pure O_2 gas with Ar. (b) Percentage variation after 1 s exposure and (c) exponential response time. The resistance does not change upon exposure to N_2, CO_2 and the inert gases Ar, He. We note that these gases, together with O_2, are the main components of air. An enhanced deintercalation rate is observed upon exposure to O_2 gas. Remarkably, the response to 20 % O_2 in Ar and to pure air (where the oxygen concentration is also approximately 20 %) is comparable, indicating that O_2 is the agent responsible for the enhanced hydrogen deintercalation rates.

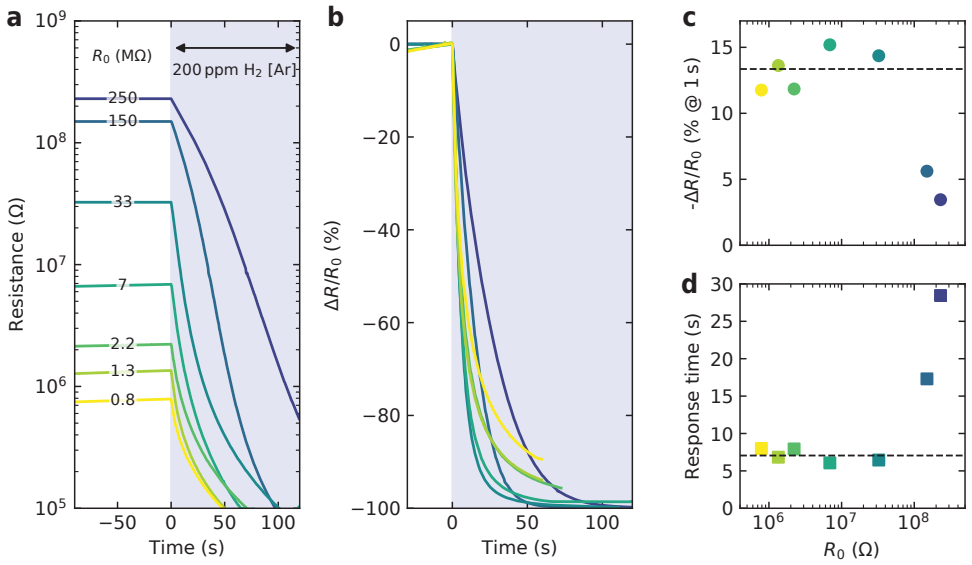

Figure S5: **Hydrogen sensing with different initial resistance.** (a) Resistance and (b) percentage variation upon exposure to 200 ppm of H_2 in Ar atmosphere with 1 bar total pressure. (c) Percentage variation after 1 s exposure and (d) exponential response time. For $R_0 < 1 \times 10^8\,\Omega$ the sensor response to 200 ppm H_2 is constant at its average value (dashed horizontal lines), within experimental error. A deviation from this is observed at the highest values of R_0, for which WO_3 is in a state of very low doping. In such state, the doping might be inhomogeneous and changes in amount of intercalated H_2 might result in smaller changes of material resistance. However, we note that the variations of the response to a fixed C_{H_2}= 200 ppm are much smaller than the ones for different C_{H_2}, so that good sensing properties are achieved independently of the value of R_0.

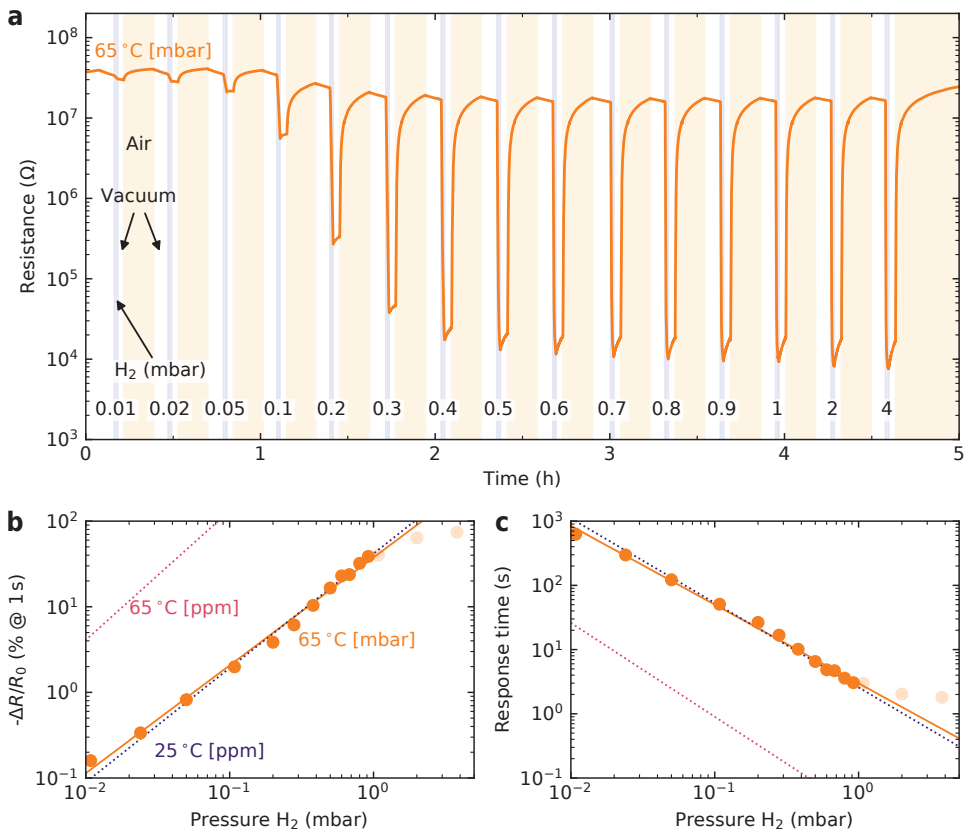

Figure S6: **Hydrogen sensing in a low-pressure H_2 blend.** (a) Resistance variations upon exposure to a mixture of 20 % H_2 in Ar, where the H_2 partial pressure is indicated in the figure. The sample is kept at 65 °C during the experiment. (b) Percentage variation after 1 s gas exposure and (c) exponential response time. The orange line is a linear fit to the experimental data. For comparison purposes, we report as dotted lines the fits relative to the ambient pressure data of Figs. 3b and 3c in the main text, where the partial pressure values are a conversion of the H_2 concentration in ppm. Because the H_2 intercalation rate is reduced at lower pressures, the WO_3 sensor shows an overall lower sensitivity to H_2 in the low-pressure regime presented here.

Model for hydrogen reaction kinetics

Intercalation We assume an infinite reservoir of hydrogen in gas phase which adsorbs on catalyst sites A, out of which a are full (molar fraction $\alpha = a/A$) and $(A - a)$ are empty. The WO_3 material has B bulk sites that can accommodate hydrogen, out of which b are full (molar fraction $\beta = b/B$). The first reaction step is irreversible (i.e. $k_{-1,\mathrm{i}} = 0$). The rates for the concentrations are:

$$\begin{cases} \dot{a} = k_{1,\mathrm{i}}(A-a)^2 + k_{-2,\mathrm{i}}b - k_{2,\mathrm{i}}a \\ \dot{b} = k_{2,\mathrm{i}}a - k_{-2,\mathrm{i}}b \end{cases} \tag{S1}$$

Transforming to molar fractions:

$$\begin{cases} \dot{\alpha} = k_{1,\mathrm{i}}A(1-\alpha)^2 + k_{-2,\mathrm{i}}\frac{B}{A}\beta - k_{2,\mathrm{i}}\alpha \\ \dot{\beta} = k_{2,\mathrm{i}}\frac{A}{B}\alpha - k_{-2,\mathrm{i}}\beta \end{cases} \tag{S2}$$

We can now assume that the system reaches a stationary condition ($\dot{\alpha} = \dot{\beta} = 0$) when $t \to \infty$:

$$\begin{cases} 0 = k_{1,\mathrm{i}}A(1-\alpha_\infty)^2 + k_{-2,\mathrm{i}}\frac{B}{A}\beta_\infty - k_{2,\mathrm{i}}\alpha_\infty \\ 0 = k_{2,\mathrm{i}}\frac{A}{B}\alpha_\infty - k_{-2,\mathrm{i}}\beta_\infty \end{cases} \tag{S3}$$

Multiplying the second equation by $\frac{B}{A}$ and summing it to the first, we find that $\alpha_\infty = 1$. From the second equation we then have $k_{2,\mathrm{i}} = \frac{B}{A}\beta_\infty k_{-2,\mathrm{i}}$. We can thus simplify the rate equations by keeping $k_{2,\mathrm{i}}$ in the first, $k_{-2,\mathrm{i}}$ in the second and using the normalised quantity $\sigma(t) = \frac{\beta(t)}{\beta_\infty}$:

$$\begin{cases} \dot{\alpha} = k_{1,\mathrm{i}}A(1-\alpha)^2 + k_{2,\mathrm{i}}(\sigma - \alpha) \\ \dot{\sigma} = k_{-2,\mathrm{i}}(\alpha - \sigma) \end{cases} \tag{S4}$$

The last set of equations can be solved numerically. We identify $\sigma(t)$ with the experimentally measured electrical conductance, normalised on its final value. This is valid with the

assumption that σ is proportional to the hydrogen concentration in the material, as discussed in the main text.

Deintercalation In this case the removal of hydrogen from WO_3 is an irreversible step (i.e. $k_{1,\mathrm{d}} = 0$) because of the vacuum atmosphere. We can write:

$$\begin{cases} \dot{a} = -k_{-1,\mathrm{d}} a^2 + k_{-2,\mathrm{d}} b - k_{2,\mathrm{d}} a \\ \dot{b} = k_{2,\mathrm{d}} a - k_{-2,\mathrm{d}} b \end{cases} \tag{S5}$$

Using molar fractions:

$$\begin{cases} \dot{\alpha} = -k_{-1,\mathrm{d}} A \alpha^2 + k_{-2,\mathrm{d}} \frac{B}{A} \beta - k_{2,\mathrm{d}} \alpha \\ \dot{\beta} = k_{2,\mathrm{d}} \frac{A}{B} \alpha - k_{-2,\mathrm{d}} \beta \end{cases} \tag{S6}$$

We consider a stationary state ($\dot{\alpha} = \dot{\beta} = 0$) before the deintercalation beginning (i.e. before the evacuation of H_2 gas), with catalyst particles saturated by hydrogen ($\alpha_0 = 1$), and some hydrogen in the WO_3 lattice ($\beta_0 > 0$). This considerations lead to $k_{2,\mathrm{d}} = \frac{B}{A} \beta_0 k_{-2,\mathrm{d}}$, which allows us to rewrite the system as:

$$\begin{cases} \dot{\alpha} = -k_{-1,\mathrm{d}} A \alpha^2 + k_{2,\mathrm{d}} (\sigma - \alpha) \\ \dot{\sigma} = k_{-2,\mathrm{d}} (\alpha - \sigma) \end{cases} \tag{S7}$$

where, as before, we take $\sigma(t) = \frac{\beta(t)}{\beta_0}$. For convenience, new rate constants can be defined as $\bar{k}_{-1,\mathrm{d}} = k_{-1,\mathrm{d}} A$ to simplify the last system. Furthermore, we note that the relation $k_{2,\mathrm{d}} = \frac{B}{A} \beta_0 k_{-2,\mathrm{d}}$ holds only for fixed values of T and p, because both A and B depend on temperature and pressure. It is thus not possible to derive the temperature dependence of $k_{2,\mathrm{d}}$ from the one of $k_{-2,\mathrm{d}}$, or vice-versa.

Model for activated electrical transport

In the following, we develop a simple thermodynamic model to express the Arrhenius activation energy for the electrical charge transport as a function of sample resistivity at $T = 300\,\mathrm{K}$. The WO_3 material is doped with hydrogen, which intercalates in the crystal lattice to form electron donor sites, such as oxygen vacancies. We consider the existence of an equilibrium for the ionisation of the donor site as

$$\mathrm{V_O^{\times}} \underset{\leftarrow}{\overset{k_{eq}}{\rightleftharpoons}} \mathrm{V_O^{\bullet\bullet}} + 2\,\mathrm{e^-}, \tag{S8}$$

where, in Kröger–Vink notation, $\mathrm{V_O^{\times}}$ represents a neutral oxygen vacancy and $\mathrm{V_O^{\bullet\bullet}}$ a double ionised one. The corresponding equilibrium constant is

$$k_{\mathrm{eq}} = \frac{[\mathrm{V_O^{\bullet\bullet}}]n^2}{[\mathrm{V_O^{\times}}]} = \frac{n^3}{2[\mathrm{V_O^{\times}}]}, \tag{S9}$$

where n is the concentration of electrons in the material and $[\mathrm{V_O^{\bullet\bullet}}] = \frac{n}{2}$ for the reaction equation. We note that here k_{eq} is an effective rate constant because it is written in terms of concentrations rather than thermodynamic activities. We can solve for the electron density

$$n = (2[\mathrm{V_O^{\times}}]k_{\mathrm{eq}})^{\frac{1}{3}}. \tag{S10}$$

In general, the concentration of donor sites will depend on the hydrogen concentration in WO_3, so that we can assume $[\mathrm{V_O^{\times}}] \sim C_{\mathrm{H}}$. Furthermore, there could be additional ionisation equilibria that affect the experimental value of n (i.e. the single ionisation of the oxygen vacancy, or the ionisation of an interstitial hydrogen radical). For this reason we generalise Eq. (S10) by introducing an exponent γ and, disregarding the constant terms, we obtain

$$n \sim (C_{\mathrm{H}}k_{\mathrm{eq}})^{\gamma}. \tag{S11}$$

We now consider that the temperature dependence of an equilibrium constant can be written as a function of the associated Gibbs free energy variation ΔG as

$$k_{\mathrm{eq}} \sim e^{-\frac{\Delta G}{k_{\mathrm{B}} T}}. \tag{S12}$$

The free energy can be expressed as

$$\Delta G = \Delta G^{\circ} + g(C_{\mathrm{H}}) = \Delta H^{\circ} - T\Delta S^{\circ} + g(C_{\mathrm{H}}), \tag{S13}$$

where ΔH° and ΔS° are, respectively, the standard enthalpy and entropy variations of the reaction, and $g(C_{\mathrm{H}})$ is a function that takes into account the non-ideality of the donor ionisation reaction, comprising, for example, the interaction between the reaction species (both electrons and donor sites). We note that, apart from $T\Delta S^{\circ}$, all terms in Eq. (S13) are temperature independent. Because the electrical conductance σ is usually proportional to the carrier density, we can write

$$\log \sigma \sim \log n = \gamma \left[\log C_{\mathrm{H}} + \log k_{\mathrm{eq}}\right] \tag{S14}$$

and substitute $\rho = 1/\sigma$ and the Eqs. (S12) and (S13) to obtain

$$\log \rho = \gamma \left[-\log C_{\mathrm{H}} - \frac{\Delta S^{\circ}}{k_{\mathrm{B}}} + \frac{\Delta H^{\circ} + g(C_{\mathrm{H}})}{k_{\mathrm{B}} T} \right]. \tag{S15}$$

Considering that C_{H} does not depend on temperature, at $T = T_0 \equiv 300\,\mathrm{K}$ we have

$$\log \rho_0 = \gamma \left[-\log C_{\mathrm{H}} - \frac{\Delta S^{\circ}}{k_{\mathrm{B}}} + \frac{\Delta H^{\circ} + g(C_{\mathrm{H}})}{k_{\mathrm{B}} T_0} \right]. \tag{S16}$$

According to the Arrhenius activated mechanism for electrical transport, which we used in the main text to describe the data of Fig. 5a, we have

$$\log \rho \sim \frac{E_{\mathrm{a}}}{k_{\mathrm{B}} T}. \tag{S17}$$

Comparing the temperature dependences of Eq. (S15) and Eq. (S17) we find

$$\gamma \frac{\Delta H^{\circ} + g(C_{\mathrm{H}})}{k_{\mathrm{B}} T} = \frac{E_{\mathrm{a}}}{k_{\mathrm{B}} T}, \tag{S18}$$

from which, substituting Eq. (S16), we obtain the following expression for the activation energy

$$E_{\mathrm{a}} = k_{\mathrm{B}} T_0 [\log \rho_0 + \gamma \log C_{\mathrm{H}}] + \gamma T_0 \Delta S^{\circ}. \tag{S19}$$

Video S1

The video shows several pictures of two identical WO_3 ultrathin films that are exposed to H_2 gas at room temperature. The sample on the left is not decorated by the Pt catalyst and does not respond to the gas. The sample on the right, instead, is decorated by 1 nm of Pt catalyst and switches from transparent ($t = 0$, undoped state) to a blue colour (doped state).